Numerical Simulations on Explosion of Leaked Liquefied Petroleum Gas in a Garage

Y.W. Ng, Y. Huo and W.K. Chow*
Department of Building Services Engineering
The Hong Kong Polytechnic University
Hong Kong, China

C.L. Chow
Department of Architecture and Civil Engineering
City University of Hong Kong
Hong Kong, China

F.M. Cheng
School of Safety Science and Engineering
Xi'an University of Science and Technology
Xi'an, China

*Corresponding author. Email: beelize@polyu.edu.hk; bewkchow@polyu.edu.hk

Acknowledgement

The work described in this article was supported by a grant from the Research Grants Council of the Hong Kong Special Administrative Region for the project "A study on explosion hazards of clean refrigerant propane leaking from air-conditioning units in small commercial flats" (PolyU 152034/14E) with account number B-Q42U and National Natural Science Foundation of China (No. 51676051).

Submitted: December 2016
Revised: February 2017

Numerical Simulations on Explosion of Leaked Liquefied Petroleum Gas in a Garage

Abstract

An explosion while repairing liquefied petroleum gas (LPG) taxis in a garage located at the ground level of an old residential building constructed in Hong Kong was reported in 2015. Part of the building structures was damaged with the owners staying inside killed. The cause of explosion is still under investigation, but the explosion source can be due to leaking of LPG fuel or flammable clean refrigerants with LPG. A taxi has over 0.5 kg of refrigerant HFC134a (R134a) stored in the air-conditioning unit. A pressure rise exceeding 21 kPa (or 0.21 bar) due to explosion from a small amount of LPG would give damages to the building. As firefighters are always exposing themselves to the risk of explosion when they are carrying out rescue operation in a gas-filled environment, the explosion overpressure has to be more reliably estimated for working out protection schemes during operation. This garage LPG explosion incident was studied numerically using Computational Fluid Dynamics software Flame Acceleration Simulation (FLACS). Three scenarios of different LPG-air mixture volumes and LPG concentrations were investigated. Dispersion of LPG was simulated first with an ignition taken at a position at the garage centre. Overpressure and temperature rise were predicted using a fine grid system with 1,657,600 computing cells was employed. Results were compared with numerical predictions using coarse grids of 207,200 cells. Discussion and conclusions were made with reference to the threshold value of 21 kPa in overpressure.

Keywords: explosion, concentration, mixture volume, transient overpressures

1. Introduction

Many gas explosions in residential buildings in big cities in the Asia-Oceania areas have been reported (Chow 2015a, 2015b). For example, over 47 gas leakage incidents were reported over the past five years by the end of November 2014 in Hong Kong. Explosion of leakage gas caused (The Sun 2015) 45 casualties including 9 firefighters. Causes of the incidents were mainly due to gas leakage unnoticed by the occupants, carelessness of workers when carrying out jobs, and suicide attempted by occupant. Many of these explosion incidents involved liquefied petroleum gas (LPG). One of the tragedies occurred (South China Morning Post 2002) in a domestic unit of a high-rise residential building in October 2002 when an occupant attempted suicide by releasing LPG. In that gas explosion, 3 women were killed and 21 people, mostly firefighters, were injured. The explosion caused severe damage to the affected unit and lift doors in the common corridor. One occupant was even killed in the opposite unit. Another gas explosion incident occurred (Lo and Nip 2013) in a Chinese restaurant of empty space volume 200 m^3 located on the first floor of a two-storey commercial complex in January 2013. Hydrocarbon clean refrigerant was involved in this explosion incident with 21 people injured and 4 of them in serious condition.

Another explosion occurred (Siu and Mok 2015) in April 2015 in a garage when repairing a LPG taxi. 3 persons including the owner were killed and 9 people were injured in this explosion. The garage was located on the ground floor of an old residential building constructed over 50 years ago. This is a typical local garage of space 200 m^3 with a rolling door at the front entrance. Part of the building structures was also damaged (Siu and Mok 2015) and the building had to be closed temporarily for structural inspection. The cause of this gas explosion is unknown and is still under investigation. In addition to having LPG fuel

in a taxi, there are flammable LPG clean refrigerants (Chow 2015b; Siu and Mok 2015). A taxi will have at least 0.5 kg of refrigerant HFC134a (R134a) in the air-conditioning unit, and might carry more gas refills. Explosion in an enclosed space without appropriate protection and detection system can result from leaking such a small amount of flammable gas.

As firefighters are always exposing themselves to the risk of explosion (Fung et al. 2014) when they are carrying out rescue operation in a gas-filled environment, the transient gas explosion pressure has to be better understood for protecting them during operation. The explosion pressure should not (Buckland 1980) exceed 21 kPa or about 0.21 bar to avoid serious damages to the building as suggested. The minimum amount of LPG required to generate 21 kPa in a garage of empty space volume 200 m^3 was estimated (Chow 2015a, 2015b) to be 3 kg. This minimum amount is less than 3 kg if the net free space, is substantially less than 200 m^3 due to the presence of objects in garage.

Accidental release of flammable gas or vapor into enclosures or the atmosphere can lead to the formation of combustible fuel-air mixtures (Catlin et al. 1995). If a suitable ignition source is present together with suitable physical conditions of confinement or congestion, explosion may occur and result in the generation of damaging overpressures in the absence of protection systems for pressure relief or fire suppression. The magnitude of the overpressures generated in explosions depends on many factors, such as the fuel, its stoichiometry, and the degree of confinement. In addition, obstacles located ahead of propagating premixed flame might generate overpressures. Experimental studies (Moen et al. 1980; Harris and Wickens 1989) demonstrated that the presence of such obstacles can increase flame speeds, and hence increase overpressures through both flame distortion effects and the establishment of a feedback mechanism between burning rate and flow field turbulence. In contrast, it has also

been shown (Moen 1982; Harris and Wickens 1989) that the continued presence of repeated obstacles is required in order to maintain high flame speeds, with flames emerging from regions containing obstacles into unobstructed volumes and then decelerating rapidly.

Over the years, mathematical models have been developed to provide realistic estimates of explosion overpressures for application in the safe design and operation of industrial plants. Computational Fluid Dynamics (CFD) has been applied for studying the development of temperature, overpressure and flame for hazard assessment involving gas explosions and fires in confined spaces (Hjertager 1982, 1993; Hjertager and Solberg 1999; Popat et al. 1996; Ogle 1999; Jo and Kim 2001; Jo and Park 2004; Paik et al. 2010; van der Heijden et al. 2013; Chiu et al. 2013; Cai and Chow 2014). Basically, conservation equations on momentum, enthalpy and mass species with some assumed chemical reactions are solved instantaneously with appropriate computational algorithms, such as the software Semi-Implicit Method for Pressure Linked Equations (SIMPLE) (Patankar 1981). The CFD software package FLame ACceleration Simulator (FLACS) (GexCon AS 2009) is a popular CFD software. Effects of turbulence on combustion were studied under complicated geometry matching with real explosion scenarios.

Since 1993, numerous validation studies have been conducted to compare the simulation results of FLACS (GexCon AS 2009) with a number of explosion experiments (http://www.gexcon.com/flacs-software/article/cfd-validation). In addition, the accuracy of the software and coefficient of the hydrocarbon premixed combustible gas flow field were validated (Skarsbø LR 2011; Bleyer et al. 2012; Davis et al. 2009; Hansen 2010; Health and Safety Laboratory 2010; Ichard et al. 2012; Middha et al. 2010; Pedersen et al. 2013 and Vyazmina 2016).

Although there is not much theoretical estimation and analysis involved in this study, some ideal assumptions have been adopted in the theoretical analysis. However, in the absence of available theoretical support and references on full-scale experiments, numerical simulations and data developed from high-efficiency explosion-proof technology, there may be a difference between the result of simulations and the actual deflagration (Walsh et al. 2016). Further experiments on in-depth understanding on the behaviour of LPG deflagration thermal flow field in a garage with a relatively large volume based on this study should be carried out.

Based on information of the case of LPG explosion in that garage taken out from public websites (Lands Department 2016; Occupational Safety & Health Council 2016) the pressure and temperature development in the garage were predicted by CFD (Hjertager 1982, 1993; Popat et al. 1996; Ogle 1999; Hjertager and Solberg 1999; Jo and Kim 2001; Jo and Park 2004; Paik et al. 2010) in this paper. FLACS is selected as the CFD simulation tool in the present study. Combustion should be modelled in explosion simulation, which might not be needed in fire simulations. This is because for fire simulation, the fire is localized, particularly in studying fire-induced air flow in very complicated geometry. In that case investigation can be focused on convective flow field far away from the fire. For explosion, fuel and air are favorably mixed and the scenario is totally different. The flaming region was then visualized by the predicted temperature contours. Results are also compared with CFD simulation using coarse grids reported before (Huo et al. 2016). Regarding the effects on the openings of the fully enclosed space due to the explosion of LPG, relevant study had previously been studied (Huo et al. 2016) and such issue will not be repeated in this paper. The results obtained in this study can help to provide a better understanding on the behaviour of LPG deflagration for risk assessment, and preventing having more LPG explosions in a garage.

2. Numerical simulations

The numerical simulation software used in the present study is FLACS (GexCon AS 2009; Huo et al. 2016). The CFD software FLACS was developed in Norway since 1980s (Hjertager 1982, 1993; Popat et al. 1996) with turbulence treated by the k−ε model. The flame is modelled by the β model, whereby the diffusion of the flame zone increases with factor β and the reaction rate decreases by 1/β. FLACS uses different mathematical approach for different stages of explosion. In the early stage of explosion such as spark ignition of a combustible cloud under quiescent conditions, FLACS models the situation with laminar burning velocity, where the flame is smooth and governed by molecular diffusion. In a short period of time after ignition, the flame becomes quasi-laminar where instability leads to the wrinkling of the flame. After the transitional period, the flame becomes turbulent and expands to a size much larger than that of the laminar due to better mixing of reactants and products. FLACS uses correlations for both laminar and turbulent burning velocities from the historical results of experiments. The wall functions are used to model the influence of the wall at a certain distance from the fire. FLACS solves the compressible conservation equations on a three-dimensional Cartesian coordinate system grid using a finite volume method. The conservation equations for mass, momentum, enthalpy and mass fraction of species are included in the ideal gas law. The numerical model uses a second-order scheme for discretization, and the time stepping scheme used in FLACS is a first-order backward Euler scheme. The SIMPLE pressure correction algorithm (Patankar 1981) is applied, and extended to handle compressible flows with additional source terms for the compression work in the enthalpy equation. Iterations are repeated until a mass residual of less than 10^{-4} is obtained. The formula and relevant numerical constants are summarized in Appendix A.

The dimensions of the garage are 8.0 m long, 7.0 m wide and 3.7 m high, as shown in Fig. 1. A Cartesian coordinate system is adopted with *x*-direction along the length, *y*-direction along the width and *z*-direction along the height.

A rolling shutter is present at the front entrance of the garage, as in the real case. The roller shutter is away from the wall by less than 0.3 m and is completely closed to give a well-sealed garage. It is assumed that there is no cracking of the door and the boundary surface of the garage due to explosion or overpressure.

The boundaries of the garage are treated according to solid wall boundary condition. The velocity vectors are zero at solid walls, both in the tangential and perpendicular directions. As the boundary layers are regions in the flow field close to walls where there are steep gradients and peak values for turbulent kinetic energy and its dissipation rate plus very close to the wall surface which dominates viscous forces over inertial effects, wall-functions (GexCon AS 2009) to model the influence of the wall at a point a certain distance from the wall is adopted in this study.

LPG vapour is highly flammable as it contains butane and propane (Occupational Safety & Health Council 2016). LPG-air mixture with LPG concentration lying between 2% and 10% by volume can be easily ignited and exploded. As LPG is stored in fuel tanks at elevated pressure, any leakage will immediately vapourise and disperse. The volume fractions of LPG in this study is taken to have 60% propane and 40% butane. Normally, a garage would not have overnight security guards. Should the leakage of LPG inside the garage be not detected or noticed for a period of time, a large amount of leaked LPG will accumulate inside the garage with sufficient time for LPG gas diffusion to mix with the air. Apart from the diffusion

process of LPG affected by obstacles, wall openings and ventilation in the garage, the location and concentration distribution of premixed gas inside the garage also create unpredictable complex situations (Dobashi 1997). Therefore, in order to simplify the complex situations of a real environment, the LPG is assumed to be mixed with air at 20^{o}C in a cube of side *a* located at the centre of the bottom of the garage to have LPG concentration of 3.6%. The density of LPG is assumed 2.12 kg/m^3. Three scenarios are simulated by taking *a* as 1 m, 1.5 m and 2 m. The corresponding volumes of the LPG-air mixtures (V1, V2, V3) are then 1 m^3, 3.375 m^3 and 8 m^3. The mixing ratio of LPG and air is within the explosive limits in the cube. To give a LPG concentration of 3.6% in these LPG-air mixtures of 1 m^3, 3.375 m^3 and 8 m^3, the mass of LPG is 0.074 kg, 0.248 kg and 0.588 kg respectively.

In this paper, LPG concentration is assumed to be distributed evenly with the stoichiometric ratio at 1. As the same amount of premixed gas explosion level is relatively intense at this point, the result of the simulations can provide some theoretical basis for designing appropriate systems for preventing and control of explosion of LPG in a garage (Pritchard et al. 1996).

These three scenarios with LPG concentration of 3.6% in the LPG-air mixture are labelled as:

V1: LPG-air mixture volume of 1 m^3, containing 0.074 kg LPG.

V2: LPG-air mixture volume of 3.375 m^3, containing 0.248 kg LPG.

V3: LPG-air mixture volume of 8 m^3, containing 0.588 kg LPG.

The ignition point is located at a height of 0.425 m above the centre of the bottom of the garage. It is assumed that the explosion occurs within 1 s after ignition.

A fine mesh dimension of 0.05 m x 0.05 m x 0.05 m is used with 160, 140 and 74 parts along *x*-, y- and *z*-direction, respectively. This gives a total number of 1,657,600 cells. A coarse grid system (Huo et al. 2016) with 207,200 cells as in Fig. 1(d) is also used for such simulation with results compared with fine grids.

3. Overpressures predicted

Simulation results showing transient overpressures P and pressure impulses I in the garage after igniting the LPG mixtures V1, V2 and V3 are given in Fig. 2. The pressure impulse I is defined by:

$$I = \int_{t1}^{t2} P \, dt \tag{1}$$

Since the ignition point is located within the LPG and air mixing zone with the same concentration, the preliminary stage of explosion in the three scenarios is similar with the pressure curve starting to rise about 0.1 s after ignition (Fig. 2(a)). The increase in pressure, however, is different. The higher the mass of the LPG, the larger is the increase in pressure.

In all three scenarios, the pressure impulse starts to rise about 0.2 s after ignition. The pressure slope of the curve increases with the mass of LPG (Fig. 2(b)).

The maximum overpressures upon LPG explosion for the three scenarios V1, V2 and V3 are shown in Fig. 3. The maximum overpressure in the three scenarios appears to form a linear relationship with the mass of LPG m_{LPG} or volume LPG-air mixture $V_{LPG+Air}$. The linear relationship is given by Equations (2) and (3) below in the present study.

$$P_{\mathrm{Max}} = 0.0545\, V_{\mathrm{LPG+AIR}} \quad (2)$$

$$P_{\mathrm{Max}} = 0.741\, m_{\mathrm{LPG}} \quad (3)$$

4. Temperature and LPG concentration

When explosion of LPG occurs in the three different scenarios, the temperature and concentration of combustible gas are respectively shown in Figs. 4 to 6. The region with high temperature can be taken as an indication of the flame patterns.

As seen from these figures, LPG is gradually consumed in the burning process after the premixed gas has been ignited. The burning process, which is dynamic, is slowing down while the concentration of LPG decreases.

Although different LPG-air mixture volume is set for the three scenarios, the LPG fuel consumed in the explosion forms a high-temperature zone in all scenarios. When the volume of the premixed gas is 1 m^3 in V1 (Fig. 4), the high-temperature zone starts to expand like a ball before 0.4 s. After 0.4 s, the high-temperature zone at the bottom part of the garage starts to contract, and the high-temperature flames start to move to the upper zone of the garage. At the same time, the LPG fuel in the middle section is nearly completely consumed at 0.3 s.

The volume of the premixed gas is 3.375 m^3 and 8 m^3 in V2 and V3 respectively (Figs. 5 and 6). Although the volumes are different from that of V1, since the concentration of the LPG fuel in V1-V3 are the same, the dynamic movement and the pattern of change of LPG fuel are essentially similar to that of V1. The only difference is the increase in volume of premixed

gas. Since there is an increase in LPG fuel, the high-temperature zone in the garage starts to contract and move to the upper part of the garage after 0.6-0.7 s. In addition, LPG fuel is completely consumed after 0.4 s.

5. Comparison of predicted results by coarse grids and fine grids

In order to understand the effects of using different scale grid on simulation results, a 0.1 m coarse grid is used for calculation. This grid is double the size of the 0.05 m fine grid. The total number of grids is reduced to 207,200 cells, with 80, 70 and 37 parts along *x*-, *y*- and *z*-direction as in Fig. 1(d). The computing times required are 95.3 hr for fine grids and 6 hr for coarse grids for V1; 106 hr for fine grids and 8.6 hr for coarse grids for V2; and 113.5 hr for fine grids and 8.7 hr for coarse grids of V3.

The transient overpressure P and pressure impulse I obtained from the coarse grid and fine grid simulations are shown in Fig. 7. As seen from the figure, the results and trends are similar for the two grid systems. The time when overpressure starts to increase is also the same, only that the maximum overpressure obtained via using the coarse grid is slightly lower than that using the fine grid. As for scenario V3 with larger volume of combustible gas, the difference between the two grid systems is more significant for the overpressure, but the pressure impulse remains similar. This indicates that the change in overpressure caused by explosion within the garage can be predicted through the coarse grid or the fine grid system. However, the predicted maximum overpressure is slightly lower using the coarse grid system. As for scenarios where the volume of combustible gas is small, the difference in the results of using coarse grids and fine grids is negligible.

For scenarios V1 to V3, the typical time when temperature starts to rise from the use of coarse grids and fine grids is shown in Fig. 8. As seen from these figures, the high temperature zones as obtained from coarse grids and fine grids are essentially the same. In using the coarse grid system, the turbulence in the enclosed space is averaged over a larger scale. Therefore, when using coarse grids, certain events of turbulence might not be effectively captured like that in the fine grid system.

The present study shows that coarse grids would provide the general pattern of explosion overpressure and high-temperature zones. More computing time is needed in the fine grid simulations (about 15.87, 12.28 and 13.09 times for scenarios V1, V2 and V3) compared with those for the coarse grid system. More accurate results can be generated with the use of finer grids (Chow and Chow 2009). Although the grid size is reduced from 0.1 m to 0.05 m in this study, the difference in the results is not obvious. However, the computation time is increased by more than 10 times through the use of finer grids. Taking into account of the hardware capability and computation time of the computers in nowadays, the smallest acceptable grid size of 0.05 m can be used. Although accurate result can be obtained through the use of a coarser grid with size of 0.1 m, the current most acceptable smallest grid of 0.05 m is used in the simulation of this study.

6. Simulation of explosions with different concentrations

In reality, apart from the effects as a result of gas leakage rate under various situations as demonstrated in the LPG dispersion tests (Brzenzinska 2016), the leaked LPG after mixing with air will form different concentrations of premixed flammable gas under the influence of openings and ventilation. Therefore, based on the typical concentration of premixed

flammable gas as a result of the different amount of leaked LPG mixing with air, this section studies the results obtained by using different concentrations of LPG within the same container. With the concentration in the previous simulation taken as 1 (that is, the reference concentration), the new relative concentrations of LPG are (a) 0.6, (b) 0.8, (c) 1.2 and (d) 1.4, and the corresponding LPG concentrations are (a) 2.2%, (b) 2.9%, (c) 4.3% and (d) 5.0%.

In summary, there are 12 new scenarios as shown below and they are simulated using the fine grid system:

For scenario V1 on LPG-air mixture volume of 1 m^3, 4 new scenarios are:

- V1-a: containing 0.045 kg LPG
- V1-b: containing 0.059 kg LPG
- V1-c: containing 0.088 kg LPG
- V1-d: containing 0.102 kg LPG

On V2 with LPG-air mixture volume of 3.375 m^3, 4 new scenarios are:

- V2-a: containing 0.151 kg LPG
- V2-b: containing 0.20 kg LPG
- V2-c: containing 0.296 kg LPG
- V2-d: containing 0.342 kg LPG

On V3 with LPG-air mixture volume of 8 m^3, 4 new scenarios are:

- V3-a: containing 0.358 kg LPG
- V3-b: containing 0.474 kg LPG
- V3-c: containing 0.701 kg LPG

- V3-d: containing 0.812 kg LPG

The overpressures and pressure impulses of different concentrations of LPG with volumes of 1 m^3, 3.375 m^3 and 8 m^3 are shown in Fig. 9. It can be observed that for the same volume of LPG-air mixture, the rise in overpressure and pressure impulse with time increases with the LPG concentration. In the overpressure rising stage, the overpressure begins to increase when the concentration of the premixed gas is close to and slightly higher than the optimum equivalent ratio (3.6%). However, the time is significantly lagging behind when the concentration of premixed gas is much less than or higher than the optimum equivalent ratio. The overpressure begins to rise at the latest when the concentration of premixed gas is only 2.2%. Such a phenomenon indicates that the development of deflagration is relatively steady. The maximum overpressures reached for different LPG-air mixtures are shown in Fig. 10. It can be observed that as the volume of the LPG-air mixture increases, the mass of LPG increases accordingly, and the maximum values of overpressure increases, almost in a linear manner and agrees well with Equation (3). The maximum overpressure value generated from the explosion is higher than 0.21 bar for LPG mass of more than 0.3 kg.

In an explosion the transient overpressure varies rapidly with time. The time instants at which the maximum slope of the increase in overpressure occurs for different concentrations of LPG and different mixture volumes are shown in Fig. 11. It can be seen that both the volume of LPG-air mixture and the LPG concentration affect the time instant at which the maximum rate of increase of overpressure occurs. As shown in Fig. 11, when the concentration of the premix LPG is 3% to 4.5%, the maximum rate of increase in the overpressure occurs within 0.3 s after the explosion starts, irrespective of the LPG-air mixture volume. It is shown that when the concentration of premixed gas is close to and slightly higher than the optimal equivalent ratio,

the maximum velocity gradient in this case occurs the earliest. When the premix gas has a volume of 1 m^3 and 3.375 m^3, the maximum increase in slope occurs at around 0.63 s at an LPG concentration of 2.2 %. As for premix gas of volume 8 m^3, the maximum increase in slope occurs at 1.3 s at an LPG concentration of 2.2 %.

Since the mass of LPG in the LPG-air mixture of scenarios V1 (1 m^3) and V2 (3.375 m^3) is relatively small compared to that of scenario V3 (8 m^3), only a small increase in overpressure and pressure impulse is observed in the explosion. However, the time of the explosion of scenarios V1 and V2 is shorter than that of the scenario V3 when the concentration of LPG is outside the optimum range of explosion (3.0 % to 4.5 %) as noted in the simulation. The reason for this phenomenon is due to the difference in concentrations of LPG in the garage and oxygen needed for combustion. Although some areas of the concentration of LPG have high explosion pressure within a short period as shown in Fig. 9, the results in Fig. 11 reflect that the fuel in the garage tends to burn with a slow combustion rate when the LPG concentration is above the optimum range of explosion.

LPG vapour is highly flammable and will easily ignite and explode when its concentration ranges from 2% to 10% in an LPG-air mixture if an ignition source is present in the vicinity. From the above results, when the concentration of LPG is within the optimum range (3.0 % to 4.5 %), the maximum rate of increase in overpressure is fast. The results also show that for the scenario of LPG-air mixture of volume 1 m^3, when the amount of combustible gas is relatively small in the space with relatively large amount of air, the combustible gas can mix with air more easily and leads to the maximum rate of increase in overpressure increasing gradually along with the increase in concentration of the premixed gas during the deflagration process. As for LPG-air mixture of volume 3.375 m^3 and 8 m^3, when the concentration of

LPG is below or beyond–the optimum range, it takes longer time to rise in overpressure, especially in the scenario with larger LPG-air mixture volume. Such observation is illustrated in the rate of rise of overpressure curves in Fig. 12.

In summary, through comparing the deflagration results of premixed gas of the same volume but with different concentrations, it is found that overpressure increases rapidly when the concentration of premixed gas is close to and slightly higher than the optimum equivalent ratio and the maximum velocity gradient occurs relatively early. However，when the concentration of premixed gas is too high or too low, the initial rapid development stage of deflagration is delayed. When the concentration of premixed gas is low, the development process of deflagration stage is relatively steady, and the magnitude of overpressure is relatively low. When the premixed gas concentration is high, the development is relatively slow at the early stage of deflagration, but the magnitude of overpressure is relatively high for a certain period of time.

7. Discussion

The explosion process resulting from igniting leaked LPG in a garage has been simulated using FLACS.

The air pressure in the garage increases after explosion for all three scenarios V1, V2 and V3. The rate of increase in overpressure is relatively slow at 0.1 s before the explosion. The high-temperature zone is small and then starts to expand spherically. Flame size denoted by high-temperature zone then increases. Suppressing the explosion at this time is effective and ideal since the hazard and destruction caused by the explosion is relatively small.

As the explosion evolves, the heat generated increases the temperature of the unburned gas and the pressure of unburned gas rises to a certain extent. This accelerates the combustion process, resulting in the exponential growth of the parameters related to overpressure.

In scenarios V1, V2 and V3, the rapid increase in pressure is sustained from 0.1 s to 0.2 s, 0.3 s and 0.4 s. As seen from the temperature and the LPG concentration at this stage, the high-temperature zone expands to give a bigger flame with the volume of the combustible gas increased. The longer this stage lasts, the larger the impact is on the garage. The pressure caused by the explosion then reaches the maximum value when most of the combustible gas has been burnt. After this stage, the high-temperature zone or the flame region resulting from explosion starts to expand to the upper part of the garage due to buoyancy.

CFD simulations show that explosion occurs within a short time after ignition in the middle part of the combustible gas. The flames then spread very quickly at a high speed. Flammable gas near to the ignition point spreads gradually to the surrounding and is eventually consumed after explosion.

While the flammable gas is being consumed, it disperses continuously from the ignition point due to the effects of explosion. The flames move to the upper part of the garage due to buoyancy. The flame region or the high-temperature zone near the bottom of the garage is slowly reduced. In the explosion, the flames develop in all directions. The rising flames are forced to move laterally after hitting the ceiling or change directions after hitting the walls of the garage.

Since the middle part of the LPG is the first area to be consumed with the surrounding air

being sucked into the rising flames, the high-temperature zone in the middle part of the flames is relatively small. The high-temperature zone in the surroundings is relatively big. In scenarios V1 and V2 with smaller amount of flammable gas, the flames develop laterally 1 s after ignition, separating the flames from the middle portion. As the explosion develops, the high-temperature zone caused by the explosion starts to form at the upper part of the garage. The bottom part of the garage is then less affected by the high-temperature flames. In the simulation in this paper, owing to the symmetry in geometry and to the position of the ignition point, the flame shape appears symmetric about the central vertical axis.

Destructive explosion occurs when the dispersed LPG form a certain mixing ratio with air. Dispersing 0.588 kg of LPG can cause a pressure rise of 0.435 bar, which is above the 0.21 bar threshold and is sufficient to bring destructive effects to a structure. In addition, Equation (3) derived in this paper suggests that 0.283 kg of LPG is required to cause an explosion pressure rise of 0.21 bar.

The simulation scenario assumes that LPG and combustible air mixture reaches the optimal equivalence ratio under the condition that all LPG is combusted. These are conditions designed for ideal combustions to take place. However, due to diffusion and ventilation in the actual testing environment, the concentration of the combustible gas formed by LPG leakage is not uniform. As a result, the explosion resulted from the ignition is very complex (Haugom and Friis-Hansen 2010).

In this study, finer grid gives better results on the simulation of using different LPG-air mixture volumes to predict the optimum range of LPG concentration and the rate of increase in overpressure after explosion, but more grid cells involve longer simulation time. From the

results of the fine grid simulation in this paper, the results are grid dependent. When a finer mesh is used, the predictions may change. More accurate predictions can be obtained in the fine grid simulation. Nevertheless, the use of coarse grid system as demonstrated in the previous study (Huo et al. 2016) could also provide a good reference to predict the phenomenon of explosion, transient pressure and pressure impulse of the explosion at different time of the leaked LPG.

8. Conclusions

The LPG explosion that occurred in April 2015 in Hong Kong due to a LPG taxi in a garage of a residential building was simulated by CFD-FLACS. The following conclusions are reached in the present study:

1. The overpressure in an explosion should not exceed 21 kPa or about 0.21 bar to avoid serious injuries/fatalities of human beings, including firefighters, and damages to the building. Based on this threshold value, the present study shows that explosion by igniting a LPG-air mixture volume of 8 m^3, with a LPG concentration of 2.2-5.0 volume %, is detrimental. For a smaller volume of mixture (3.375 m^3), the threshold is exceeded for LPG concentrations ≥4.3 volume %. For mixture volume of 1 m^3, the maximum overpressure is below 0.1 bar for LPG concentrations in the range 2.2-5.0 volume %.

2. For the three LPG-air mixture volumes, the shortest time for the occurrence of the maximum rate of increase in overpressure is around 0.25 s, at a LPG concentration in the range 3%-4.5%.

3. After comparing the results of the coarse grid and fine grid simulations, it is found that the results and trends are similar for both of the two grid systems. However, the coarse grid system will slightly under-estimate the maximum overpressure and certain events of turbulence might not be effectively captured like that in the fine grid system, including change of LPG concentration under combustion, development of high-temperature zone, burning pattern and heat distribution.

Predicted results are expected to be useful for hazard assessment associated with gas explosions while firefighters are carrying out rescue operation in a gas-filled environment. Better understanding of explosion overpressure would assist fire officers to decide whether they are able to send firefighters to the site for carrying out rescue and fire suppressions operations.

Appendix: A Summary of FLACS

The mathematical model for compressible fluid flow used in FLACS mainly includes:

Conservation of mass:

$$\frac{\partial}{\partial t}\left(\beta_v \rho\right)+\frac{\partial}{\partial x_j}\left(\beta_j \rho u_j\right)=\frac{\dot{m}}{V} \tag{A1}$$

Momentum equation:

$$\frac{\partial}{\partial t}\left(\beta_v \rho u_i\right)+\frac{\partial}{\partial x_j}\left(\beta_j \rho u_i u_j\right)=-\beta_v \frac{\partial p}{\partial x_i}+\frac{\partial}{\partial x_j}\left(\beta_j \sigma_{ij}\right)+F_{o,i}+\beta_v F_{w,i}+\beta_v\left(\rho-\rho_0\right) g_i \tag{A2}$$

Transport equation for enthalpy:

$$\frac{\partial}{\partial t}\left(\beta_v \rho h\right)+\frac{\partial}{\partial x_j}\left(\beta_j \rho u_j h\right)=\frac{\partial}{\partial x_j}\left(\beta_j \frac{\mu_{\mathrm{eff}}}{\sigma_h} \frac{\partial h}{\partial x_j}\right)+\beta_v \frac{Dp}{Dt}+\frac{\dot{Q}}{V} \tag{A3}$$

Transport equation for fuel mass fraction:

$$\frac{\partial}{\partial t}\left(\beta_v \rho \gamma_{\mathrm{fuel}}\right)+\frac{\partial}{\partial x_j}\left(\beta_j \rho u_j \gamma_{\mathrm{fuel}}\right)=\frac{\partial}{\partial x_j}\left(\beta_j \frac{\mu_{\mathrm{eff}}}{\sigma_{\mathrm{fuel}}} \frac{\partial \gamma_{\mathrm{fuel}}}{\partial x_j}\right)+R_{\mathrm{fuel}} \tag{A4}$$

Transport equation for the mixture fraction:

$$\frac{\partial}{\partial t}\left(\beta_v \rho \xi\right) + \frac{\partial}{\partial x_j}\left(\beta_j \rho u_j \xi\right) = \frac{\partial}{\partial x_j}\left(\beta_j \frac{\mu_{\text{eff}}}{\sigma_\xi}\frac{\partial \xi}{\partial x_j}\right) \tag{A5}$$

Transport equation for turbulent kinetic energy:

$$\frac{\partial}{\partial t}\left(\beta_v \rho k\right) + \frac{\partial}{\partial x_j}\left(\beta_j \rho u_j k\right) = \frac{\partial}{\partial x_j}\left(\beta_j \frac{\mu_{\text{eff}}}{\sigma_k}\frac{\partial k}{\partial x_j}\right) + \beta_v P_k - \beta_v \rho \varepsilon \tag{A6}$$

Transport equation for the dissipation rate of turbulent kinetic energy:

$$\frac{\partial}{\partial t}\left(\beta_v \rho \varepsilon\right) + \frac{\partial}{\partial x_j}\left(\beta_j \rho u_j \varepsilon\right) = \frac{\partial}{\partial x_j}\left(\beta_j \frac{\mu_{\text{eff}}}{\sigma_\varepsilon}\frac{\partial \varepsilon}{\partial x_j}\right) + \beta_v P_\varepsilon - C_{2\varepsilon}\beta_v \rho \frac{\varepsilon^2}{k} \tag{A7}$$

Here $F_{w,i}$ is flow resistance due to walls and $F_{o,i}$ is flow resistance due to sub-grid obstructions:

$$F_{o,i} = -\rho \left|\frac{\partial \beta}{\partial x_i}\right| u_i \left|u_i\right| \tag{A8}$$

The stress tensor σ_{ij} is given by:

$$\sigma_{ij} = \mu_{\text{eff}}\left(\frac{\partial u_i}{\partial x_j} + \frac{\partial u_j}{\partial x_i}\right) - \frac{2}{3}\delta_{ij}\left(\rho k + \mu_{\text{eff}}\frac{\partial u_k}{\partial x_k}\right) \tag{A9}$$

The effective viscosity is defined as follows:

$$\mu_{\text{eff}} = \mu + \mu_t = \mu + \rho C_\mu \frac{k^2}{\varepsilon} \tag{A10}$$

In each of the formula above, t is time; β_v is volume porosity; ρ is density; $\dot{m}$ is mass rate; V is volume; u is mean velocity; β_j is area porosity in the j th direction; p is absolute pressure; g is gravitational acceleration; h is specific enthalpy; $\dot{Q}$ is heat rate; γ_{fuel} is mass fraction of fuel; R_{fuel} is reaction rate for fuel; ξ is mixture fraction; k is turbulent kinetic energy; ε is dissipation of turbulent kinetic energy; μ is dynamic viscosity; μ_t is dynamic turbulent viscosity.

Flow shear stresses, G_s, wall shear stresses, G_w, and buoyancy, G_b contribute to the production of turbulent kinetic energy P_k:

$$P_k = G_s + G_w + G_b \tag{A11}$$

The production rate of turbulent kinetic energy due to shear stresses appears from the derivation of the transport equation and reads:

$$G_s = \sigma_{ij} \frac{\partial u_i}{\partial x_j} \tag{A12}$$

Buoyant forces obtained by a simple gradient model are given by:

$$G_b = -\frac{1}{\rho} \frac{\mu_{\text{eff}}}{\sigma_b} g_i \frac{\partial \rho}{\partial x_i} \tag{A13}$$

Dissipation P_ε is modelled as follows:

$$P_\varepsilon = C_{1\varepsilon}\frac{k}{\varepsilon}P_k\left(1+C_{3\varepsilon}R_f\right) \tag{A14}$$

where the model for the buoyancy term is：

$$R_f = -\frac{G_b}{P_k}\frac{\left|\vec{u}\times\vec{g}\right|}{\left|\vec{u}\right|\left|\vec{g}\right|} \tag{A15}$$

In FLACS, the buoyancy terms G_b and R_f are assumed to be zero when products are present.

A few constants are included in the equations mentioned above. In FLACS, the following set of constants is used: C_μ is 0.09; $C_{1\varepsilon}$ is 1.44; $C_{2\varepsilon}$ is 1.92; $C_{3\varepsilon}$ is 0.8. In addition, the set of turbulent Prandtl-Schmidt numbers are: σ_h is 0.7; σ_{fuel} is 0.7; σ_ξ is 0.7; σ_k is 1.0; σ_ε is 1.3; σ_b is 0.9.

References

Bleyer A, Taveau J, Djebaili-Chaumeix N, Paillard CE, Bentaib A (2012). Comparison between FLACS explosion simulations and experiments conducted in a PWR Steam Generator casemate scale down with hydrogen gradients. *Nuclear Engineering and Design*, 245: 189-196.

Brzezinska D (2016). Safety concept for underground garages open for cars powered by LPG – results of real scale tests. 11th International Conference on Performance-Based Codes and Fire Safety Design Methods, May 23-25 2016, Warsaw.

Buckland CG (1980). Explosions of gas layers in a room size chamber. *Chemical Process Hazards VII – Institution of Chemical Engineers*, 289-304.

Cai N, Chow WK (2014). Numerical studies on heat release rate in a room fire burning wood and liquid fuel. *Building Simulation*, 7(5): 511-524.

Catlin CA, Fairweather M, Ibrahim SS (1995). Predictions of turbulent, premixed flame propagation in explosion tubes. *Combustion and Flame*, 102(1): 115-128.

Chiu Chen-Wei, Chen Chin-Hui, Chen Jia-Ci, Shu Chi-Min (2013). Analyses of smoke management models in TFT-LCD cleanroom. *Building Simulation*, 6(4): 403-413.

Chow CL, Chow WK (2009). Fire safety aspects of refuge floors in supertall buildings with computational fluid dynamics, *Journal of Civil Engineering and Management*, 15:3, 225-236.

Chow WK (2015a). Gas explosion in residential buildings to watch. Department of Building Services Engineering, The Hong Kong Polytechnic University, January 2015. Available at: http://www.bse.polyu.edu.hk/researchCentre/Fire_Engineering/Hot_Issues.html

Chow WK (2015b). Alerting gas explosions in buildings: LPG as fuel or for air-conditioner? Department of Building Services Engineering, The Hong Kong Polytechnic University, July 2015. Available at: http://www.bse.polyu.edu.hk/researchCentre/Fire_Engineering/Hot_Issues.html

Davis SG, Hansen OR, Ichard M (2009). Validation of FLACS for Vapor Dispersion from LNG Spills: Model Evaluation Protocol. 2009 International Symposium.

Dobashi R (1997). Experimental study on gas explosion behaviour in enclosure. *Journal of Loss Prevention Industries*. 10-2: 83-89.

Fung FWY, Ng J, Cheung E, Mok D (2014, November 23). 'It was like thunder': residents describe gas blast that killed one and left firemen fighting for their lives. *South China Morning Post.* http://www.scmp.com/news/hong-kong/article/1646119/firefighters-residents-injured-kowloon-explosion?page=all

GexCon AS (2009). FLACS v9.0 User's Manual. Bergen, Norway.

Hansen OR, Gavelli F, Ichard M, Davis SG (2010). Validation of FLACS against experimental data sets from the model evaluation database for LNG vapor dispersion. *Journal of Loss Prevention in the Process Industries*, 23: 857-877.

Harris RJ, Wickens MJ (1989). Understanding Vapour-Cloud Explosions - An Experimental Study. The Institution of Gas Engineers 55th Autumn Meeting, Communication 1408.

Health and Safety Laboratory (2010). Review of FLACS 9.0, Health and Safety Executive, The Government of United Kingdom.

Haugom GP, Friis-Hansen P (2010). Risk modelling of a hydrogen refuelling station using Bayesian network. *International Journal of Hydrogen Energy*, 36(3): 2389-2397.

Hjertager BH (1982). Simulation of transient compressible turbulent reactive flows. *Combustion Science and Technology*, 27: 159-170.

Hjertager BH (1993). Computer modelling of turbulent gas explosions in complex 2D and 3D geometries. *Journal of Hazardous Materials*, 34(2): 173-197.

Hjertager BH, Solberg T (1999). A review of computational fluid dynamics (CFD) modelling of gas explosions. In: Zarko VE et al. (eds), Prevention of Hazardous Fires and Explosions. Netherlands: Kluwer Academic Publishers, pp. 77-91.

Huo Y, Ng YW, Chow WK (2016). A study on gas explosions in buildings: LPG as fuel or for air-conditioner? Paper presented at CLIMA2016, 22-25 May 2016, Aalborg, Denmark.

Ichard, M, Geiser, J. & Gavelli, F (2012). CFD simulation of the Falcon tests using the homogeneous equilibrium model in FLACS. Eight Global Congress on Process Safety, 1-4 April 2012, Houston, Texas: 16 pp.

Jo YD, Kim JY (2001). Explosion hazard analysis in partially confined area. *Korean Journal of Chemical Engineering*, 18(3): 392-296.

Jo YD, Park KS (2004). Minimum amount of flammable gas for explosion within a confined space. *Process Safety Progress*, 23(4): 321-329.

Lands Department (2016). http://www1.map.gov.hk/gih3/view/index.jsp. Accessed 3 January 2016.

Lo C, Nip A (2013, January 10). Fireball rips through Ma On Shan restaurant, injuring 21. *South China Morning Post*. http://www.scmp.com/news/hong-kong/article/1124086/fireball-rips-through-ma-shan-restaurant-injuring-21.

Middha P, Hansen OR, Grune J, Kotchourko A (2010). CFD calculations of gas leak dispersion and subsequent gas explosions: validation. *Journal of hazardous Materials*, 179: 84-94.

Moen IO (1982). In: Lee JHS, Guirao CM (eds), Fuel-Air Explosions. Waterloo: University of Waterloo Press, pp. 101-135.

Moen IO, Donato M, Knystautas R, Lee JHS (1980). Flame acceleration due to turbulence produced by obstacles. *Combustion and Flame*, 39: 21-32.

Occupational Safety & Health Council, Hong Kong (2016). LPG Safety. Available at http://www.oshc.org.hk/download/publishings/1/302/36.htm. Accessed 3 January 2016.

Ogle RA (1999). Explosion hazard analysis for an enclosure partially filled with a flammable gas. *Process Safety Progress*, 18(3): 170-177.

Paik JK, Kim BJ, Jeong JS, Kim SH, Jang YS, Kim GS, Woo JH, Kim YS, Chun MJ, Shin YS, Czujko J (2010). CFD simulations of gas explosion and fire actions. *Ships and Offshore Structures*, 5(1): 3-12.

Patankar S.V. (1981). Numerical Heat Transfer and Fluid Flow. New York: McGraw Hill.

Pedersen HH, Tomlin G, Middha P, Phylaktou HN, Andrews GE (2013). Modelling large-scale vented gas explosions in a twin-compartment Enclosure. *Journal of Loss Prevention in Process Industries*, 26: 1604-1615.

Popat NR, Catlin CA, Arntzen BJ, Lindstedt RP, Hjertager BH, Solberg T, Saeter O, van den Berg AC (1996). Investigations to improve and assess the accuracy of computational fluid dynamic based explosion models. *Journal of Hazardous Materials*, 45(1): 1-25.

Pritchard DK, Freeman DJ, Guilbert PW (1996). Prediction of explosion pressures in confined spaces. *Journal of Loss Prevention Industries*. 9-3: 205-215.

Siu P, Mok D (2015, April 27). Garage explosion in Wong Tai Sin leaves three dead, nine injured. *South China Morning Post*. http://www.scmp.com/news/hong-kong/article/1776965/garage-explosion-wong-tai-sin-leaves-three-dead-five-injured

Skarsbø LR (2011). An Experimental Study of Pool Fires and Validation of Different CFD Fire Models. A thesis submitted in partial fulfilment of the requirements for the degree of Master of Science in the subject of Physics. Process Safety Technology, Department of Physics and Technology, University of Bergen, Bergen Norway.

South China Morning Post (2002, 31 October). 3 die as blast trigger fireball in tower block.

The Sun (2015, January 8). 47 gas leakage fire and explosion within 5 year.

van der Heijden MGM, Loomans MGLC, Lemaire AD, Hensen JLM (2013). Fire safety assessment of semi-open car parks based on validated CFD simulations. *Building Simulation*, 6(4): 385-394.

Walsh BP, Snodgrass RE, Black WZ (2016). Thermodynamic Model for Gas Explosions in Vented and Non-Vented Enclosures. *Combustion Science and Technology*.

Vyazmina E, Jallais S (2016). Validation and recommendations for FLACS CFD and engineering approaches to model hydrogen vented explosions: Effects of concentration, obstruction vent area and ignition position. *International Journal of Hydrogen Energy*, 41: 15101-15109.

Figure Captions

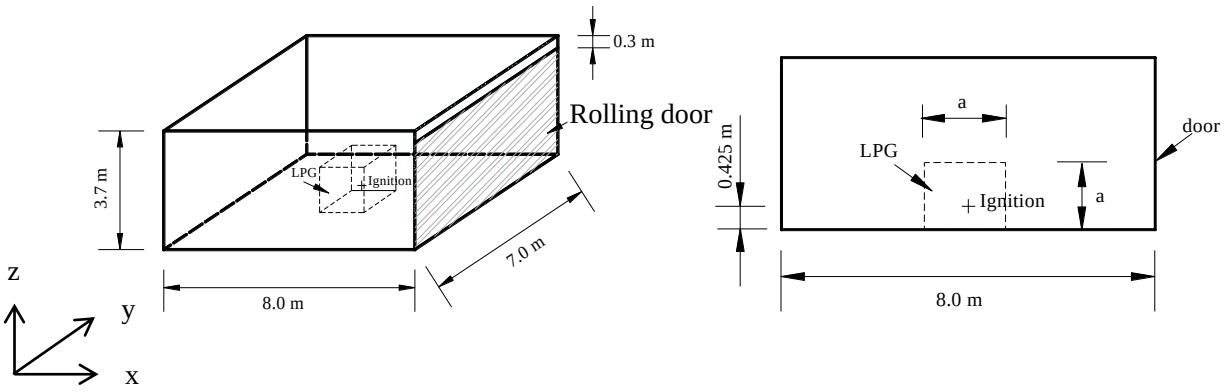

(a) Schematic drawing (b) Central vertical z-x plane

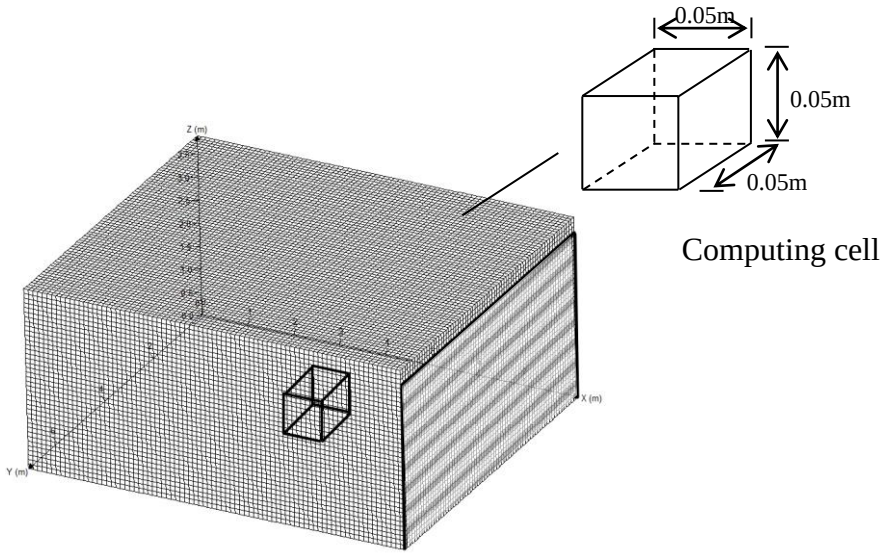

(c) Fine grid system with 1,657,600 cells

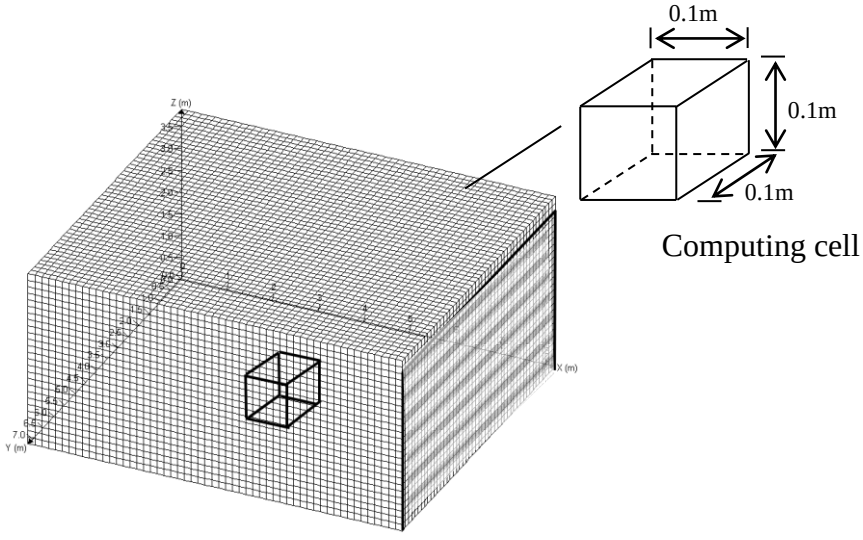

(d) Coarse grid system with 207,200 cells

Figure 1: The garage

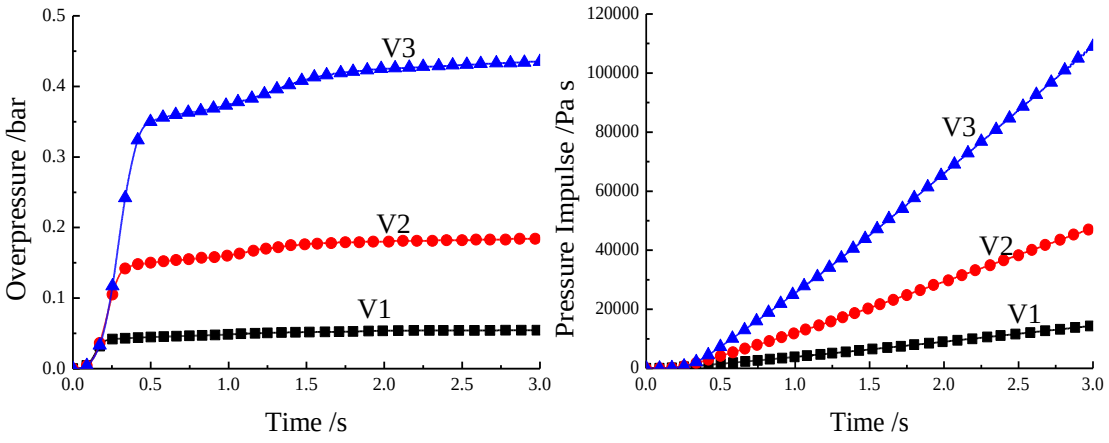

(a) Overpressure (b) Pressure impulse

Figure 2: Transient overpressure and pressure impulse for the three explosion scenarios

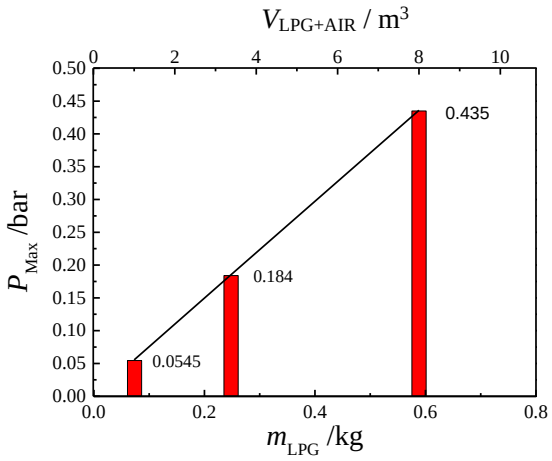

Figure 3: Maximum overpressures at different LPG volumes

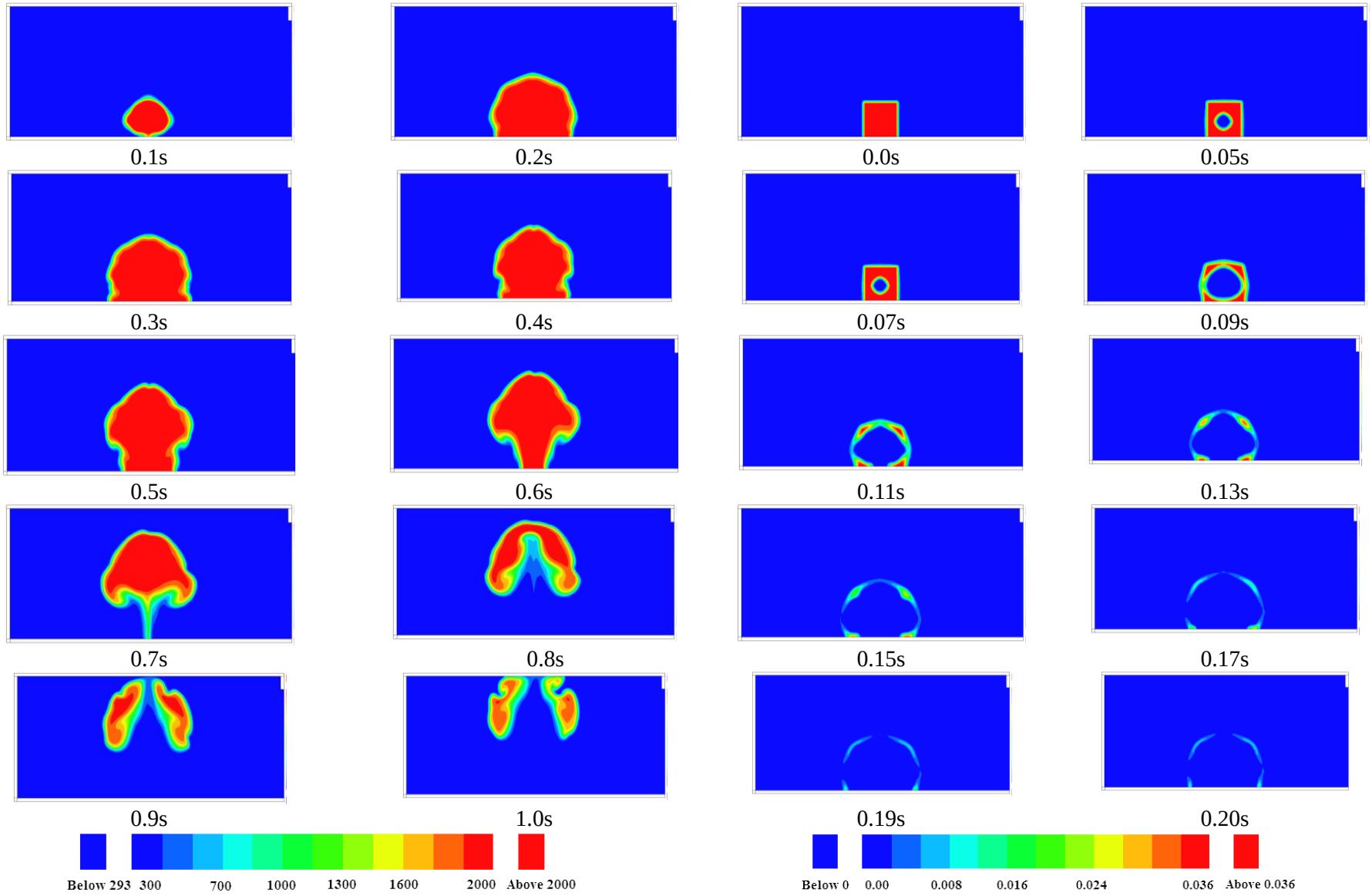

(a) Temperature rise

(b) Change in LPG concentration

Figure 4: Results for V1

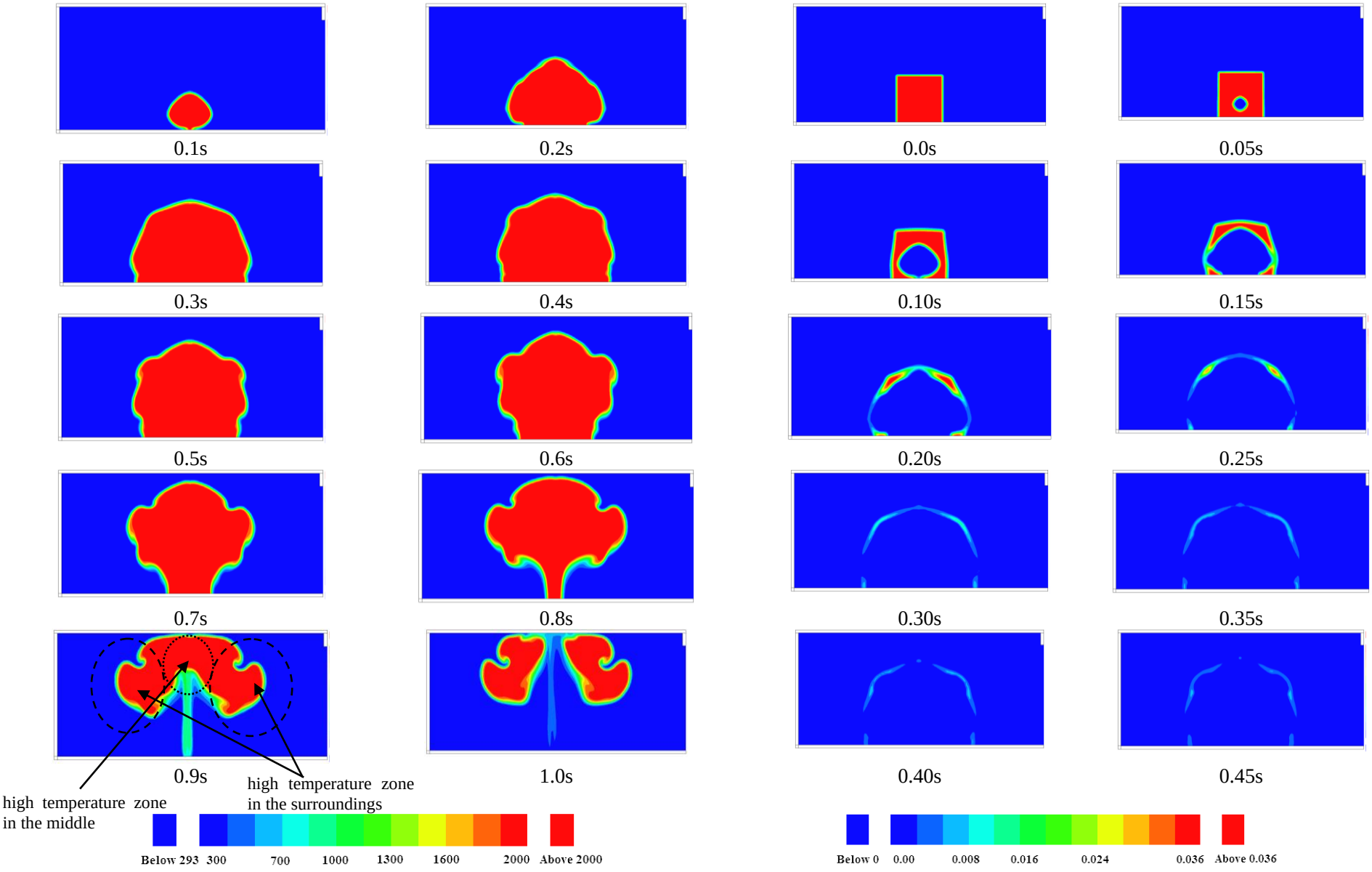

(a) Temperature rise

(b) Change in LPG concentration

Figure 5: Results for V2

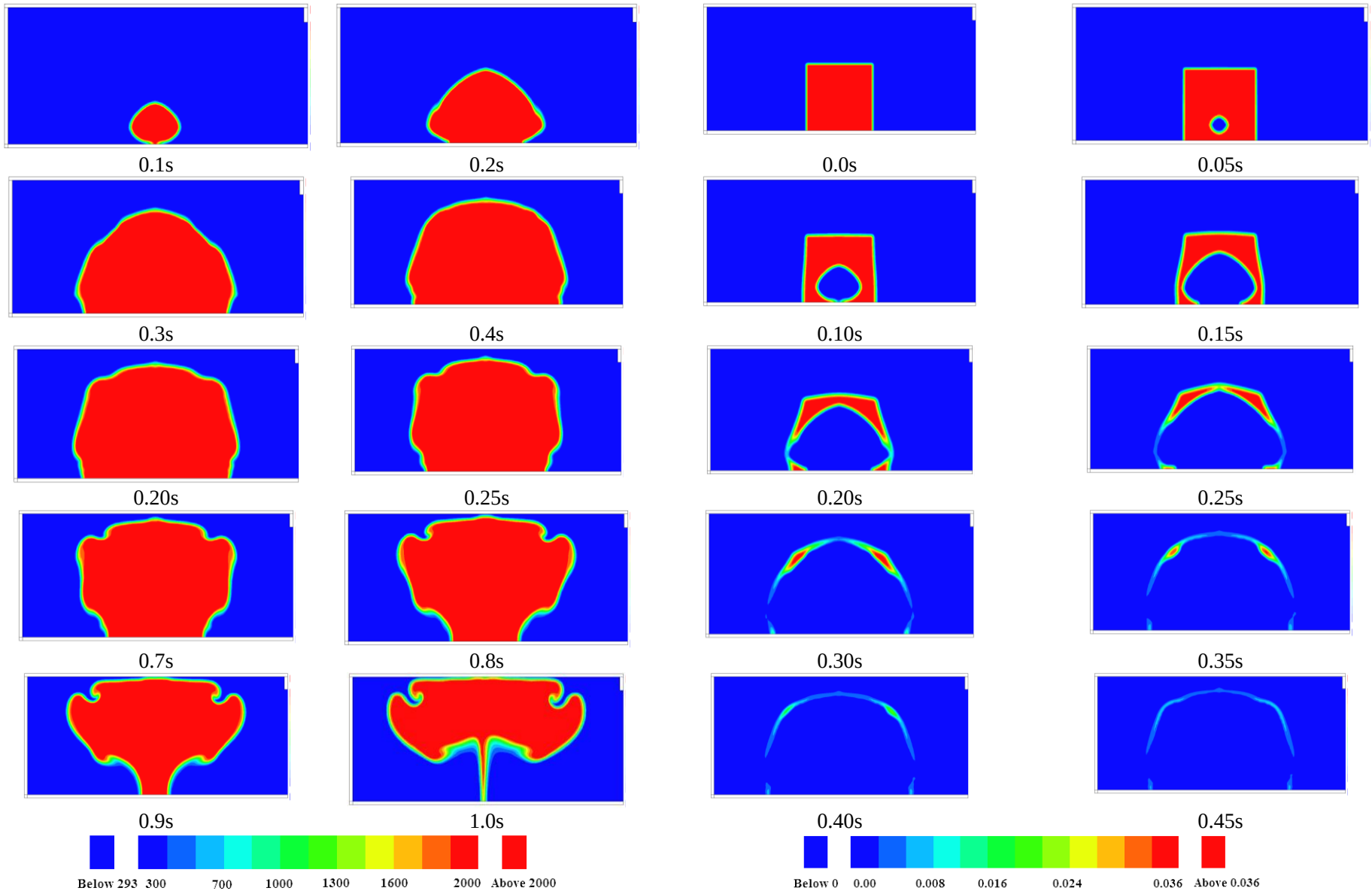

Temperature rise

Change in LPG concentration

Figure 6: Results for V3

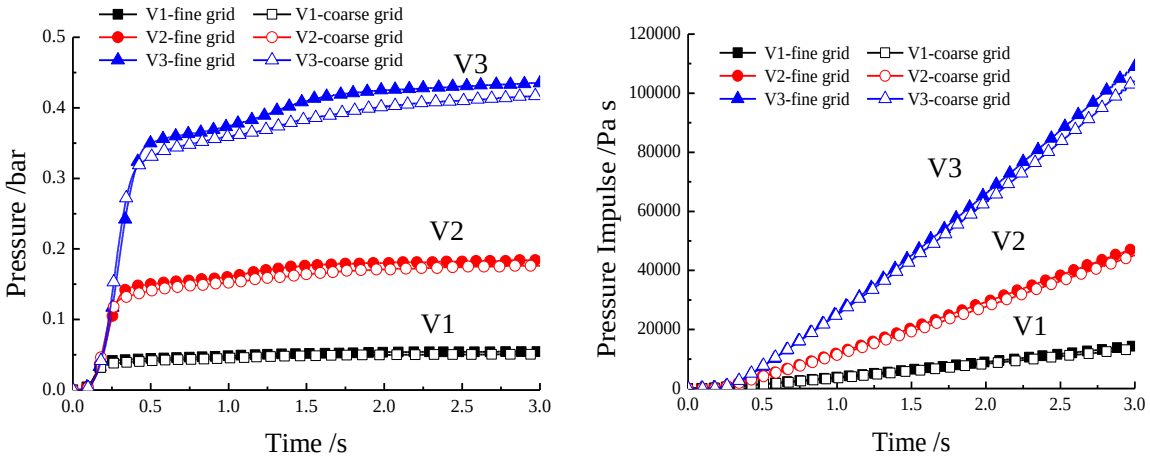

Figure 7: Transient overpressure and pressure impulse obtained from using different grids in three explosion scenarios

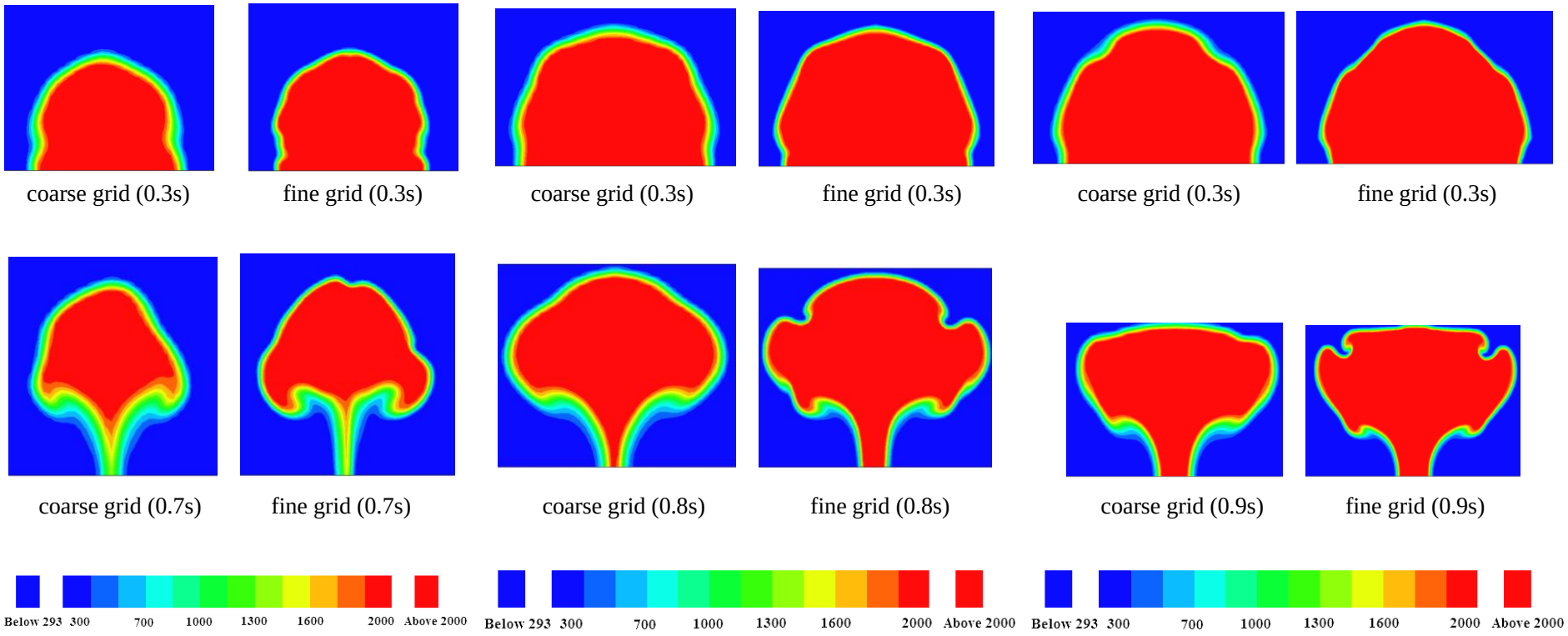

(a) Scenario V1 (b) Scenario V2 (c) Scenario V3

Figure 8: Typical temperature rise predicted

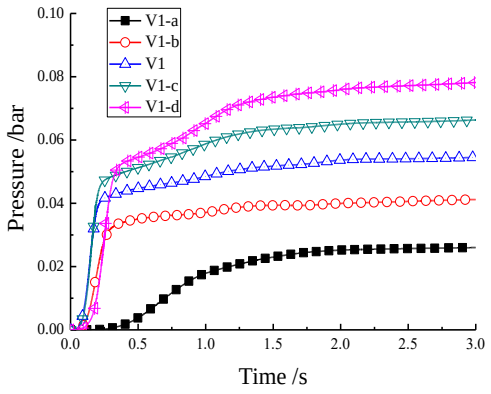

Pressure

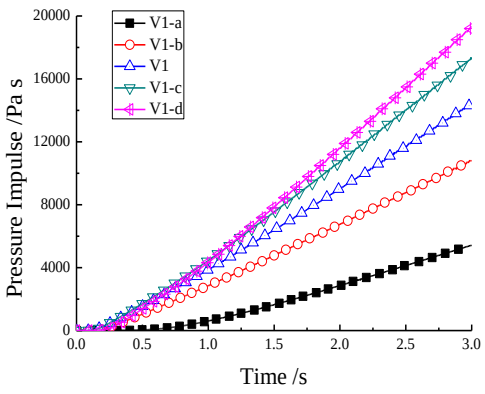

Pressure impulse

(a) 1 m^3

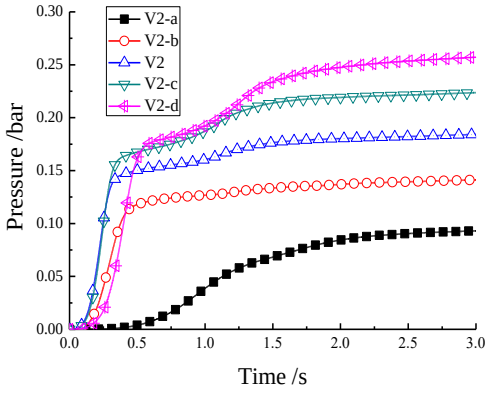

Pressure

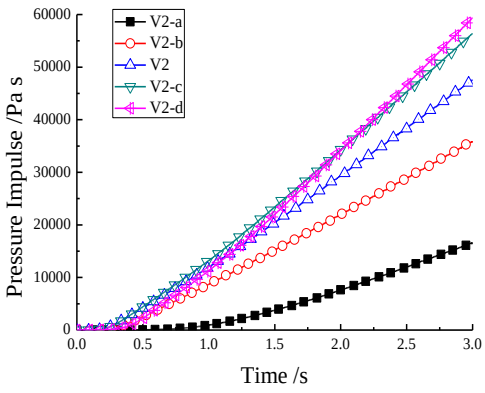

Pressure impulse

(b) 3.375 m^3

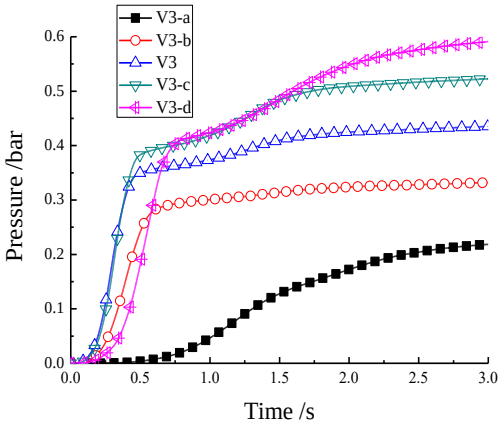

Pressure

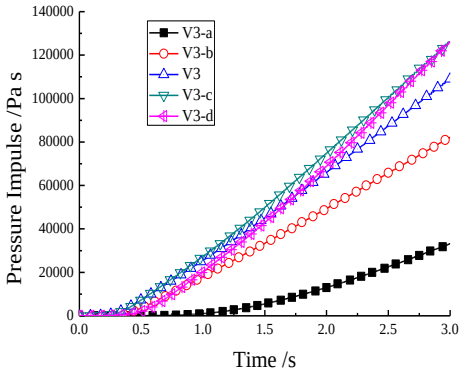

Pressure impulse

(c) 8 m^3

Figure 9: Transient overpressure and pressure impulse for premixed gas of different initial concentrations

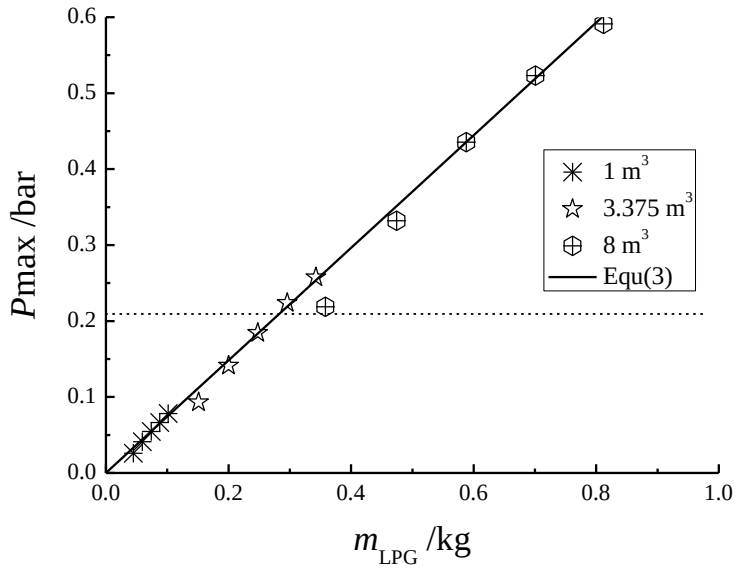

Figure 10: Maximum overpressure generated by different masses of LPG

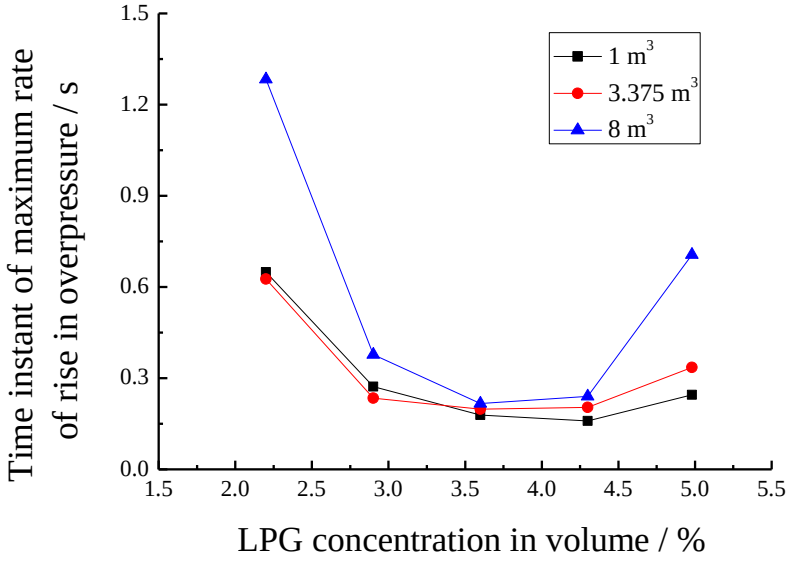

Figure 11: Time of maximum rate of increase in overpressure under different LPG concentrations

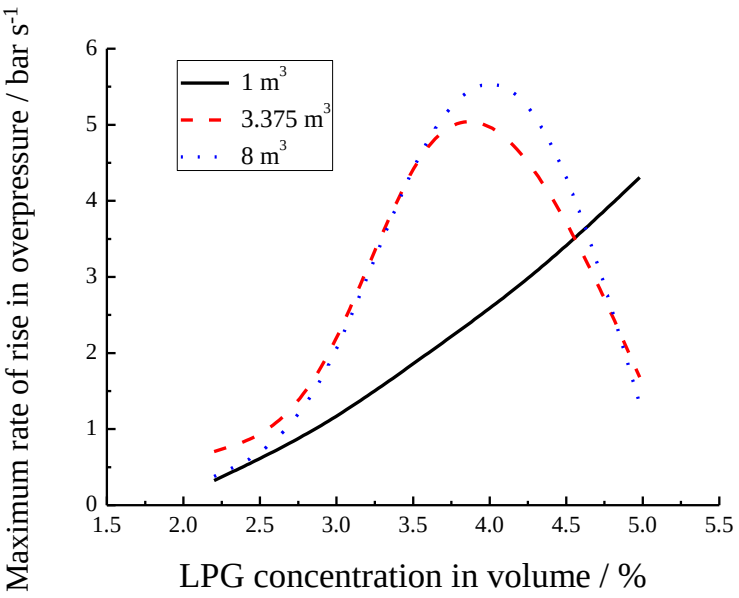

Figure 12: Maximum rate of rise in overpressure under different LPG concentrations